

Hybrid Quantum algorithm to classify Hermitian matrix definiteness

Andrés Gómez¹ and Javier Mas²

¹Centro de Supercomputación de Galicia (CESGA)

² Departamento de Física de Partículas, Universidade de Santiago de Compostela and Instituto Galego de Física de Altas Enerxías (IGFAE)

September 8th, 2020

We present a hybrid algorithm that accomplishes the classification of a Hermitian matrix according to its signature into three classes (positive semi-definite, negative or indefinite). The algorithm is probabilistic but shows good performance and scalability, at least equal to that of the pure classical counterpart. The quantum part of the hybrid algorithm uses Quantum Phase Estimation to store the eigenvalues of a Hermitian matrix in the states of a set of ancilla qubits, one of which is reserved to store the sign. The signature is extracted from the mean value of a spin operator in this single ancillary qubit.

1 Introduction

The apparent computational power due to the intrinsic parallelism of the Quantum Computing paradigm comes at the expense of the difficulty in retrieving the output state. In order to design advantageous quantum algorithms the emphasis shifts towards finding the right question to ask. Classification problems stand out as particularly suited, whereby low number of qubit measurements will suffice to discriminate and identify the correct answer. The paradigmatic example is the Deutsch algorithm and variants thereof. The second best case occurs when the measurement outcome can be shown to peak sharply around the searched solution, and accuracy can be systematically improved by enhancing some ancillary system. Quantum Phase Estimation belong to this later class. One important classification problem, associated to the spectrum of a Hermitian matrix ($M = M^\dagger \in C^{N \times N}$), is related to its definiteness, defined in terms of the sign of the quadratic form $S = \mathbf{x}^T M \mathbf{x}$. Concretely, if:

- If $S \geq 0, \forall \mathbf{x} \in C^N$ then M is termed *positive semi-definite*. Equivalently, all eigenvalues λ_i are nonnegative, $\forall i = 1, \dots, N$. The form S is positive, $S > 0$, if and only if, $\lambda_i > 0, \forall i = 1, \dots, N$, that is the matrix is *positive definite*.
- If $S \leq 0, \forall \mathbf{x} \in C^N$ then M is termed *negative semi-definite*. Equivalently, all the eigenvalues $\lambda_i \leq 0, \forall i = 1, \dots, N$. The form S is negative, $S < 0$, if and only if $\lambda_i < 0, \forall i = 1, \dots, N$, that is, the matrix is *negative definite*.
- In any other case the matrix M is *indefinite*, and the spectrum contains both positive and negative eigenvalues.

Andrés Gómez: agomez@cesga.es

Javier Mas: javier.mas@usc.es

Signature definiteness of a Hermitian operator is an important property with deep mathematical and physical impact. In optimisation algorithms when the Hessian matrix is used [1] it permits to know if the current solution is a local minimum (if the Hessian is positive definite), a local maximum (negative definite) or a saddle point (indefinite). Also positive semi-definiteness is one of the distinguishing features of a *bona fide* quantum density matrix.

Classical methods to obtain the definiteness of a M are known in the literature. The Sylvester's criterion [2] asserts that a Hermitian M is positive definite if *all* N leading principal minors are positive. However, to classify it as positive semi-definite, this characteristic is not enough, and *all* principal minors¹ must be shown to be positive [3]. This implies considerable more effort, needing the evaluation of $2^N - 1$ determinants, each one demanding $O(N!)$ operations, which can be reduced to $O(N^3)$ by, for example, Gaussian elimination. Another approach is the Cholesky's decomposition [1], which also works only if M is positive. Again, the computational complexity is $O(N^3)$. Finally, the obvious possibility is to calculate by brute force all the eigenvalues, which can be done in $O(N^w \log_2(N))$ operations [4]. The lowest bound known to date is $w = 2.376$, but practical problems demand a value higher than $\log(7) = 2.808$. This classical theoretical scaling bound will be the benchmark in our search for quantum advantage.

The hybrid algorithm presented in this paper consist of two parts. A fast classical preprocessing stage that, if sucessfull, will identify the definiteness of M in $O(N^2)$ steps. As we will show, the rate of success for this part is roughly 65%. For the remaining cases in which this method fails, we propose a quantum algorithm that shows competitive performance. The outcome is not deterministic, but peaked around the correct answer with an accuracy that increases with the depth n of the ancillary system. With $n = 14$ an overall performance over 97% of correct classification is achieved.

The quantum algorithm is based on the Quantum Phase Estimation (QPE) algorithm [5] where only one qubit of the ancillary system is inspected. Measuring $\langle \sigma_z \rangle$ on the designated qubit, M will be positive semi-definite (negative definite) iff $\langle \sigma_z \rangle = 1$ (-1) and indefinite for $\langle \sigma_z \rangle \in (-1, 1)$. Let n be the depth of the ancillary system. When the product $2^n \lambda_i$ has a nonzero mantisa for at least one eigenvalue λ_i , the statement remains the same, but the outcome of $\langle \sigma_z \rangle$ will only reveal the correct definiteness in a probabilistic sense, whose accuracy can be enhanced arbitrarily by increasing n .

The paper is divided in four sections. The first one summarises the Quantum Eigenvalue Estimation algorithm for unitary operators. The extension to Hermitian matrices is addressed in the second section. The full hybrid algorithm is spelled out in section three. Being a probabilistic method, the performance is presented as the results of simulations in the fourth section. We wrap up with some comments and outlooks.

2 Quantum Phase Estimation algorithm on the Real line

In this section we shall review the QPE algorithm with a slight twist that embodies the core of the proposal. Let $|u\rangle$ be an eigenstate of a unitary operator U . Unitarity implies that all the eigenvalues must be pure phases

$$U|u\rangle = e^{i2\pi\theta}|u\rangle. \quad (1)$$

¹The k -th leading principal minor $\Delta_k, k = 1, \dots, N$ is obtained from M by deleting the last $N - k$ rows and columns. Principal minors $D_k, k = 1, \dots, 2^N - 1$, are instead obtained by deleting *any* $N - k$ rows and columns.

Although in principle $\theta \in \mathbf{R}$ is a real number, the equivalence relation $\theta \sim \theta + k, k \in \mathbf{Z}$ allows to find a unique representative of the equivalence class in the fundamental domain $\tilde{\theta} \in [0, 1)$. The QPE algorithm provides an approximation, $x \in [0, 1)$, of order n to $\tilde{\theta}$ in the following sense: after initializing the circuit with the state $H|0\rangle^{\otimes n} \otimes |u\rangle$ the output state, $|\Phi\rangle$, will have the ancillary part set in a superposition of the computational basis $|x\rangle, x \in (0, \dots, 2^n - 1)$.

$$|\Phi\rangle = \frac{1}{2^n} \sum_{x=0}^{2^n-1} \sum_{k=0}^{2^n-1} e^{-\frac{2\pi i k}{2^n}(x-2^n\theta)} |x\rangle \otimes |u\rangle \quad (2)$$

From here, the probability of measuring a particular state $|x\rangle$ in the n -ancilla register is given by $p_n(x, \theta) = |\langle x|\Phi\rangle|^2$. If $2^n\theta$ is an integer, $p_n(x, \theta) = \delta_{x, 2^n\theta}$, and the ancillary state $|2^n\theta\rangle$ is retrieved deterministically. Otherwise, the resulting probability distribution

$$p_n(x, \theta) = \frac{1}{2^{2n}} \left| \frac{\sin \pi(2^n\theta - x)}{\sin(\pi(2^n\theta - x)/2^n)} \right|^2 \quad (3)$$

peaks sharply around the integer part $a = \text{Floor}[2^n\theta]$. Figure 1 shows the dependence of this probability distribution on the number of qubits of ancilla register. Notice that this distribution has two features. First, it decays symmetrically on both sides of a , the relative width shrinking rapidly with n . On the other, extending its domain to the full set of integers, $x \in \mathbf{Z}$, $p_n(x, \theta)$ has the shift periodicity $p_n(x, \theta) = p_n(x + 2^n k, \theta)$. This has an important consequence for values of θ , very close to the edge limits of the interval $[0, 1)$. When this happens, one side of the tail of the distribution may cross the limits, 0 or 1. By the shift symmetry, this tail reappears at the opposite edge of the interval, hence giving significant probability to a large systematic identification error.

This brings us to the key observation. Let us assume that some, otherwise unknown phase θ , is said to take value in the interval $\theta \in [-0.5, 0.5)$. Initially, for simplicity, we shall also assume that $2^n\theta \in \mathbf{Z}$ is an integer. Now: if θ belongs to the positive semi-definite subinterval $\theta \in [0, 0.5)$ then $\tilde{\theta} = \theta$ and the QPE algorithm will naturally retrieve the n -th order approximation $x = 2^n\tilde{\theta} \in [0, 2^{n-1})$. In this case, the most relevant qubit in $|x\rangle$ will always be in state $|0\rangle_{n-1}$. On the contrary, if θ belongs to the negative subinterval $\theta \in [-0.5, 0)$, the QPE will produce an approximation for the equivalent representative $\tilde{\theta} = \theta + 1 \in [0.5, 1)$. In this case $x = 2^n\tilde{\theta} \in [2^{n-1}, 2^n - 1)$ will be such that the most relevant ancillary qubit in $|x\rangle$ will be in state $|1\rangle_{n-1}$. In summary, for values of $\theta \in [-0.5, 0.5)$ such that $2^n\theta \in \mathbf{Z}$ the eigenvalues ± 1 of σ_z acting on the most significant ancillary qubit correlate exactly with $\text{sign}(\theta)$. For obvious reasons, we will refer to the subintervals $[0, 0.5)$ and $[0.5, 1)$ where the representative $\tilde{\theta}$ can belong as sign-subintervals.

In realistic case, it will not occur that $2^n\theta \in \mathbf{Z}$ for the width n of the ancillary circuit we can afford. In this case, as commented before, the outcome x follows a probability distribution which is sharply peaked around $a = \text{Floor}(2^n\theta)$. Concerning the possibility of retrieving $\text{sign}(\theta)$, we will face two types of situations. The dangerous one occurs when θ is close to either 0 or ± 0.5 . In any of these three cases, part of a side tail in the probability distribution may cross these limits, giving chances to obtaining values of x in the wrong sign-subinterval, hence with the opposite sign to that of θ . Turning the argument around, values of θ sufficiently detached from the boundaries, 0 and ± 0.5 will be such that both side tails of $p(x)$ will fit completely within the sign-subinterval where $2^n\theta$ belongs. Let us stress that this pathology is inherited from the QPE protocol itself. In that case only the values $\theta \sim 0, 1$ were weak, in the sense of producing unreliable values of x . Now, for the sign, all four possibilities for $\theta \sim 0, \pm 0.5, 1$ are fragile, in that the signs that we retrieve are prone to misidentification.

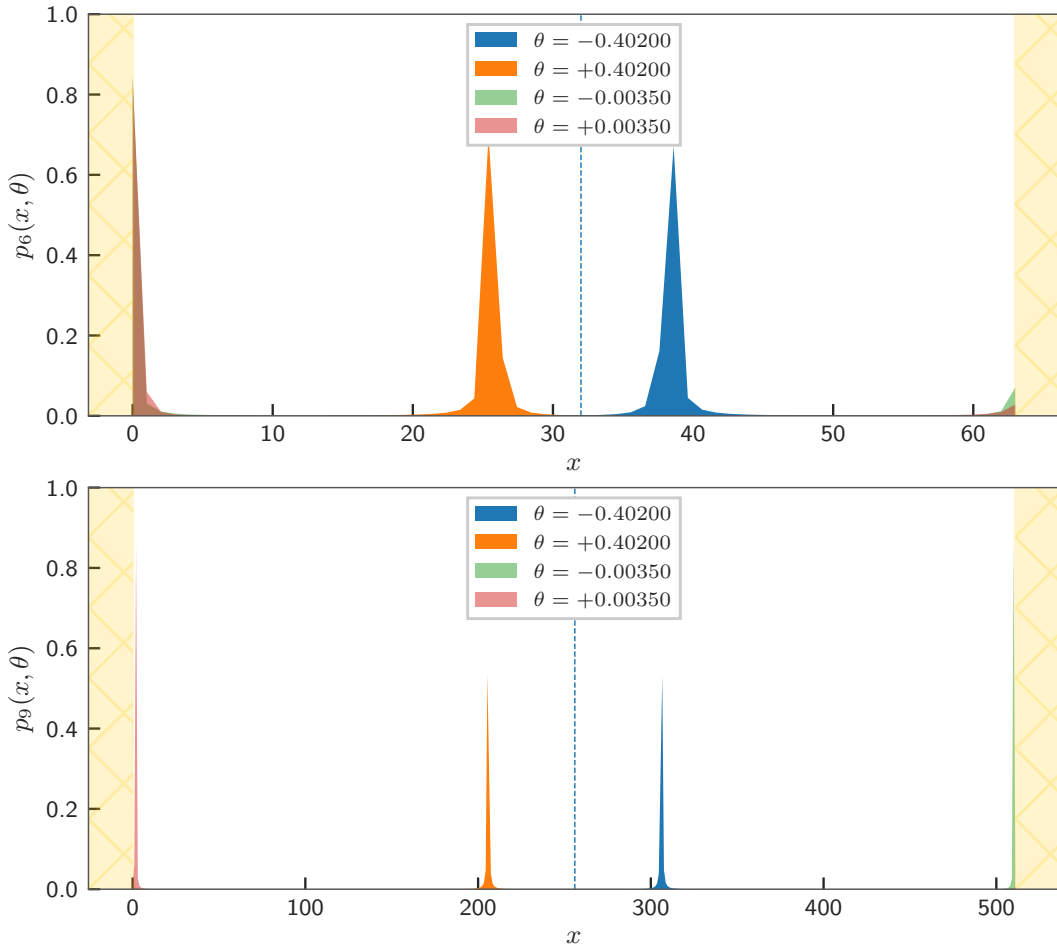


Figure 1: Probability function $p_n(x, \theta)$, of measuring the different states of the n -qubit ancilla register in the QPE algorithm for $n = 6$ and $n = 9$. The value $\theta = 0.00035$ is close to 0, and there is a substantial probability of producing a large error in x . By increasing n from 6 to 9 the peaks sharpen enough to fit completely inside the same sign-subinterval as that of θ . The brown color in the first plot comes from the overlap of the green and pink curves

An important extension we need to address encompasses the situation when U is a unitary $N \times N$ matrix, with $N = 2^m$. In some orthonormal basis $|u_i\rangle$, $i = 0, \dots, 2^m - 1$, the unitary operator acts diagonally $U = \text{diag}(e^{i2\pi\theta_0}, \dots, e^{i2\pi\theta_{N-1}})$ for an ensemble of phases $\{\theta\} = (\theta_0, \dots, \theta_{N-1})$. The idea is to initialize the QPE circuit with a normalized vector $|b\rangle$ which, generically, will have overlap with all the vectors of the eigenbasis, i.e.

$$|b\rangle = \sum_{i=0}^{N-1} \beta_i |u_i\rangle. \quad (4)$$

with $\beta_i \neq 0 \forall i = 0, \dots, N-1$. At the circuit's outlet, we will now find the following highly entangled state

$$|\Phi\rangle = \sum_{i=0}^{N-1} \frac{\beta_i}{2^n} \sum_{x=0}^{2^n-1} \sum_{k=0}^{2^n-1} e^{-\frac{2\pi i k}{2^n} (x - 2^n \theta_i)} |x\rangle \otimes |u_i\rangle \quad (5)$$

which contains a double superposition of orthonormal vectors. Therefore the probability of finding a particular ket $|x\rangle$ is given by

$$p_n(x, \{\theta\}) = \sum_{i=0}^{N-1} |\beta_i|^2 p_n(x, \theta_i) \quad (6)$$

which satisfies $\sum_x p_n(x, \{\theta\}) = 1$ consistently. This is nothing but a normalized sum over distributions of the form (3) peaked at the different values of $2^n \theta_i$, $i = 0, \dots, N-1$. A retrieval of the ensemble of phases $\{\theta\} = \theta_i$, $i = 0, \dots, N-1$ requires therefore a statistical sampling.

Regarding the signs, let us come back to the assumption that $\forall i$, $\theta_i \in [0, 0.5]$ as well as $2^n \theta_i \in \mathbf{Z}$. Then it is clear that all the states $|x\rangle$ in the superposition (5) will have the most significant qubit in state $|x\rangle_{n-1} = |0\rangle$. Equivalently, the expectation value of $\langle \sigma_z^{(n-1)} \rangle \equiv \langle \Phi | \sigma_z \otimes I^{\otimes m+n-1} | \Phi \rangle = 1$. The same conclusion can be reached for negative $\theta_i \in [-0.5, 0] \forall i$, now yielding $\langle \sigma_z^{(n-1)} \rangle = -1$. Conversely, any value of $|\langle \sigma_z^{(n-1)} \rangle| < 1$ in the most significant qubit signals the fact that the ensemble of phases, θ , does not have a globally well defined sign. Summarizing, the expectation value $\langle \sigma_z^{(n-1)} \rangle$ allows to discriminate among three possibilities related to the sign distribution of the set of phases θ_i .

When $2^n \theta$ has a nonvanishing mantisa, the above certainties turn into a distributional probability of finding either $|0\rangle$ or $|1\rangle$ when measuring the most significant ancillary qubit $|x\rangle_{n-1}$. Since all the states in (5) are orthonormal, this is obtained by simply marginalizing over all values of x compatible with $x_{n-1} = 0$ or 1 . Turning these probabilities into expectation values of $\sigma_z^{(n-1)}$ measured on the most significant qubit we arrive at

$$\langle \sigma_z^{(n-1)} \rangle = \sum_{x=0}^{2^{n-1}-1} p_n(x, \{\theta\}) - \sum_{x=2^n-1}^{2^n-1} p_n(x, \{\theta\}) \quad (7)$$

For the case of a single phase, $N = 1$, Figure 2 shows the value of (7) as a function of θ for different number of qubits in the ancilla, n . Increasing n makes the curve tend to a perfect step function that discriminates sharply between negative and positive values of θ .

Before analysing numerically this expression, let us finish the argument that is advertised in the title of this paper.

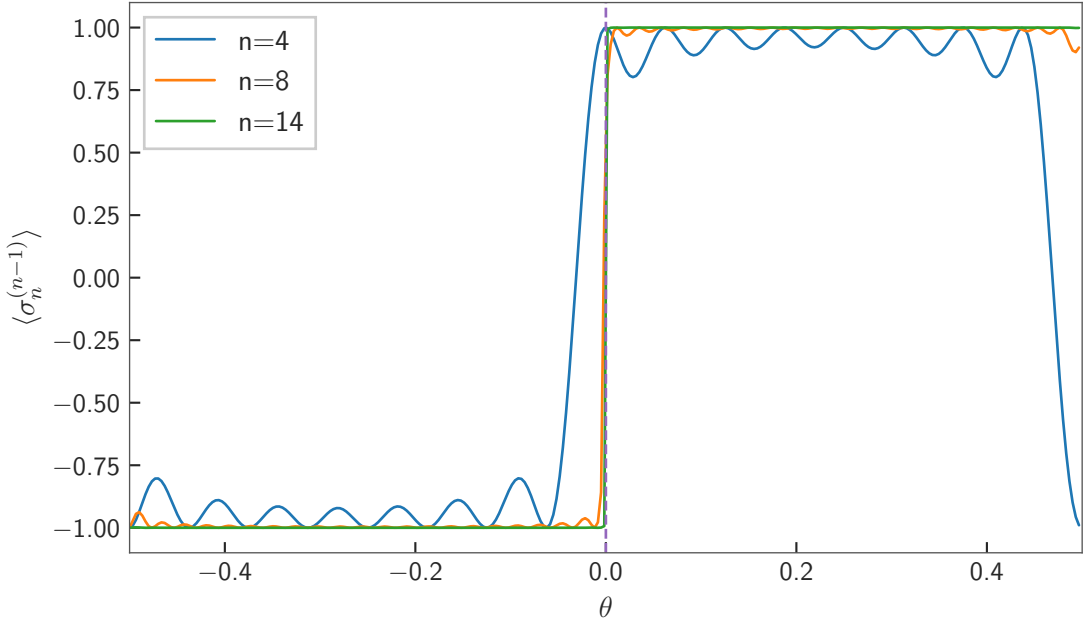


Figure 2: $\langle \sigma_z^{(n-1)} \rangle$ vs the value of a single eigenvalue eigenvalue for different number of qubits on the ancilla, following equation (7). For large n the curve tends to a step function jumping at 0.

3 Quantum Eigenvalue Estimation for Hermitian matrices

A hermitian matrix $M \in C^{N \times N}$ has N real eigenvalues $\lambda_i \in \mathbf{R}$, with eigenvectors $\{|v_i\rangle, i = 0, \dots, 2^m - 1\}$ which can be arranged to form a orthonormal basis. Hereafter we will assume that $N = 2^m$. Other cases can be treated as well by padding enough rows and columns with zeroes. We will comment on this case later.

The unitary operator $U_M = e^{iMt}$ has the same eigenvectors $|v_i\rangle$ as M , with eigenvalues $\gamma_i = e^{i\lambda_i t}$ instead. Hence the action of U_M on an arbitrary vector $|b\rangle$ is

$$U_M|b\rangle = \sum_{i=0}^{2^m-1} \beta_i U_M|v_i\rangle = \sum_{i=0}^{2^m-1} \beta_i e^{it\lambda_i} |v_i\rangle. \quad (8)$$

The QPE algorithm maps values of $\theta_i = \lambda_i t / 2\pi$ onto states of an ancillary register. Now comes the key observation: writing $t = \frac{2\pi}{C}$, the constant C can be cranked up to achieve $\forall i \rightarrow \theta_i = \lambda_i / C \in [-0.5, 0.5]$. This brings us back to the arena explored in the previous section where the most significant ancillary qubit carries (with high probability) the information about the sign of θ_i .

Let us digress now around the way to adjust conveniently the constant C , given the fact that the eigenvalues of M are not known *a priori*. All we need is an upper bound on their absolute values that allows to select C such that $|\lambda_i / C| < 0.5 \ \forall i$. In [6] Wolkowicz and Styan derived bounds for the highest and lowest eigenvalues, λ_{high} and λ_{low} respectively, of an arbitrary matrix only in terms of its trace. Let us define the quantities

$$r = \frac{\text{Tr}(M)}{N} \quad , \quad s^2 = \frac{\text{Tr}(M^2)}{N} - r^2. \quad (9)$$

The following bounds are proven for λ_{low}

$$C_{low}^{\min} \leq \lambda_{low} \leq C_{low}^{\max}, \quad (10)$$

with

$$C_{low}^{min} = r - s\sqrt{N-1} \quad , \quad C_{low}^{max} = r - \frac{s}{\sqrt{N-1}} , \quad (11)$$

and similarly for λ_{high}

$$C_{high}^{min} \leq \lambda_{high} \leq C_{high}^{max} , \quad (12)$$

with

$$C_{high}^{min} = r + \frac{s}{\sqrt{N-1}} \quad , \quad C_{high}^{max} = r + s\sqrt{N-1} . \quad (13)$$

Hence all we need to do is compute some traces. Notice that, for M a Hermitian matrix:

$$Tr(M^2) = \sum_{i,j} (M \odot M^T)_{ij} , \quad (14)$$

which reduces to $O(N^2)$ the complexity of this operation. Now clearly, choosing

$$C = 2 \operatorname{Max}(|C_{low}^{min}|, |C_{high}^{max}|) , \quad (15)$$

all the phases will satisfy

$$|\theta_i| = \left| \frac{\lambda_i}{C} \right| \leq 0.5 . \quad (16)$$

Summarizing: in what concerns our original problem, the important fact is that θ_i inherits the sign of λ_i and, more importantly, all negative (positive semi-definite) eigenvalues $\lambda_i < 0$ ($\lambda_i \geq 0$) have been mapped onto the semi-interval $\theta_i \in [-0.5, 0)$ ($\theta_i \in [0, 0.5)$).

4 Hybrid algorithm for classification of Hermitian matrices

Putting together all the previous results, we can formulate the hybrid algorithm as a two stage protocol. Given a Hermitian matrix M , in order to classify it according to its definiteness

1. perform a classical check making use of the bounds in eqs. (10) and (12). The subroutine that performs this task is shown in Algorithm 1. If this classical test fails proceed with step 2.
2. If M could not be classified classically, proceed with the quantum part, which is summarized in Algorithm 2.

The classical step makes use of equations (10) to (13). In simple words, if $C_{low}^{min} > 0$ ($= 0$), then it is clear that for all $i \rightarrow \lambda_i > 0$ ($\lambda_i \geq 0$). Hence the matrix can be classified as positive definite (positive semi-definite). Conversely, if for $C_{high}^{max} < 0$ ($= 0$), then all the eigenvalues are $\lambda_i < 0$ (≤ 0) and M will be classified as as negative definite (negative semi-definite). Finally, if both $C_{low}^{max} < 0$ and $C_{high}^{min} > 0$ are satisfied, there will be at least two eigenvalues with opposite sign, ranking M as indefinite.

Outside these situations the character of M cannot be identified without ambiguity by means of this fast classical method and the quantum algorithm described in the previous section must be used. As explained before, the essence of the quantum approach proceeds in two steps. From the initial matrix M , whose eigenvalues are λ_i , $i = 1, \dots, 2^m$, by a suitable rescaling we can obtain another one $\tilde{M} = M/C$ whose eigenvalues belong to the desired range $\theta_i = \lambda_i/C \in [-0.5, 0.5]$. The definiteness of \tilde{M} and M are the same. As for \tilde{M} , such definiteness is obtained with high probability from the measurement of $\langle \sigma_z^{(n-1)} \rangle$. Let us expand a little bit on details of both steps.

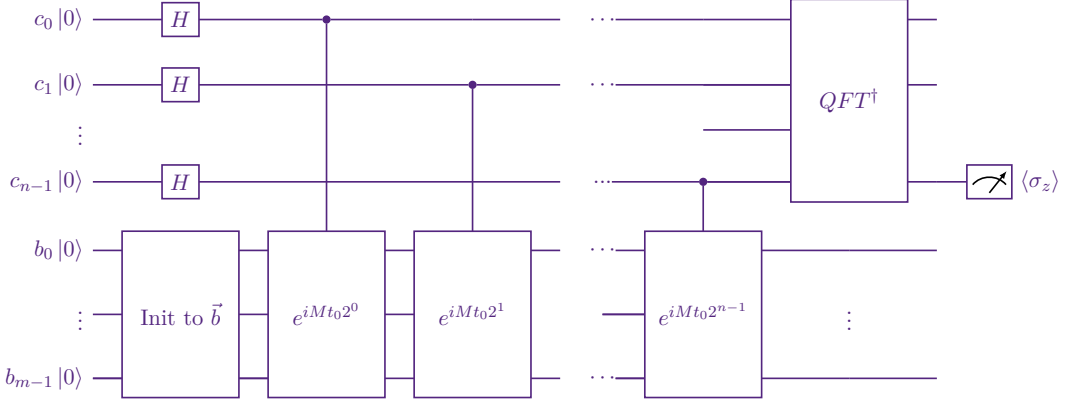


Figure 3: Quantum circuit used to calculate the definiteness of an Hermitian matrix M

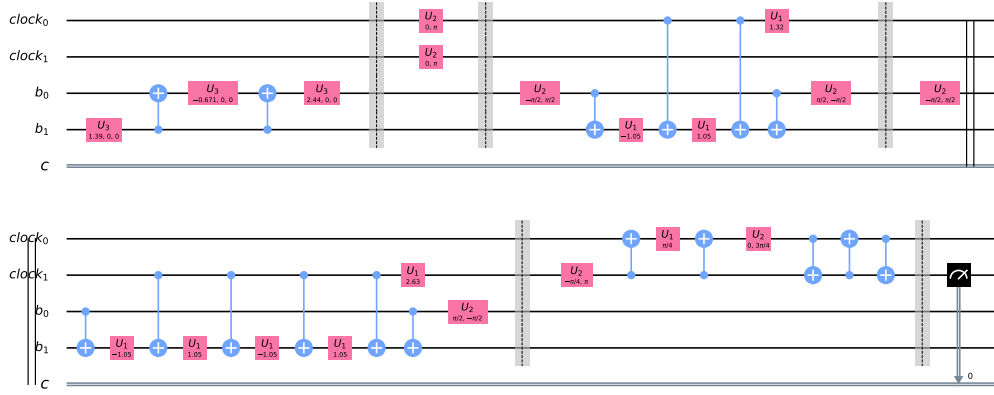


Figure 4: Transpiled circuit example for 2 ancilla qubits using Qiskit. The *Standard* version of the inverse of the Quantum Fourier Transform was used, with swapping, measuring c_{n-1} . If other inverses of QFT are used, the algorithm must take into account the final order of the qubits on the ancilla register.

In what concerns the first part, namely the rescaling, all we need to know is the constant C . Here is where the job done before for the classical stage is reusable and C will be given by the expression (15). At a practical level, as mentioned in eq. (8) this constant is included in the algorithm in the selection of the Hamiltonian evolution time step

$$U(t_0) = \exp(it_0 M) \quad (17)$$

by setting $t_0 = 2\pi/C$.

In what concerns the computation of $\langle \sigma_z^{(n-1)} \rangle$, its reliability hinges upon two factors. The first one is the accuracy, which is linked with the number of qubits, n , in the ancillary system. Increasing n squeezes the probability distribution for the outcome x , as explained in Fig. 1, in such a way that it fits almost completely within the same sign-subinterval as that associated with the original eigenvalue $\theta \rightarrow 2^n \tilde{\theta}$. The second one is the state $|b\rangle$. In order to capture all the signs, it must be initialized so that its has a nontrivial projection onto all the basis eigenvectors $|v_i\rangle$. Using a single random initialization of $|b\rangle$, there is a high probability that the decomposition includes all of them, but this is not assured. In fact, as we will show, with a single initialization, the possibility of wrong classification is high. So, the strategy is to make several trials with different initial random vectors, and calculate the average of the results for decision making. The final classification will hence

Algorithm 1: Classical check of definiteness of a matrix M using its trace. Note that when M is classified as positive semi-definite or negative semi-definite, the classification must be considered as candidate to be of this class. See text for more details about.

Input: $M \in \mathbf{C}^{N \times N}$ Hermitian Matrix
Output: Flag with class or error.
 Low and high limits for the Eigenvalues of the Matrix M

```

if  $M \neq M^\dagger$  (up to atol) then
    return Error
// Initialize internal variables
 $N \leftarrow \text{dimension}(M)$ 
 $r \leftarrow \text{using (9)}$ 
 $t \leftarrow \text{Tr}(M^2)$  using (14)
 $s \leftarrow \text{using (9) and } t$ 
 $\text{limitLowMin} \leftarrow r - s\sqrt{N-1}$ 
 $\text{limitHighMin} \leftarrow r - \frac{s}{\sqrt{N-1}}$ 
 $\text{limitLowMax} \leftarrow r + \frac{s}{\sqrt{N-1}}$ 
 $\text{limitHighMax} \leftarrow r + s\sqrt{N-1}$ 
// Classify
if  $\text{limitHighMax} < 0$  then
  |  $\text{classM} \leftarrow \text{Flag Negative Definite}$ 
else
    if  $\text{limitHighMax} \leq 0$  then
    |  $\text{classM} \leftarrow \text{Flag Negative Semi-Definite}$ 
    else
        if  $\text{limitLowMin} > 0$  then
      |  $\text{classM} \leftarrow \text{Flag Positive Definite}$ 
        else
            if  $\text{limitLowMin} \geq 0$  then
        |  $\text{classM} \leftarrow \text{Flag Positive Semi-Definite}$ 
            else
                if  $(\text{limitHighMin} < 0) \& (\text{limitLowMax} > 0)$  then
          |  $\text{classM} \leftarrow \text{Flag Indefinite}$ 
                else
          |  $\text{classM} \leftarrow \text{Flag Unclassified}$ 
      
return  $\text{classM}, \text{limitLowMin}, \text{limitHighMax}$ 

```

depend upon a threshold which we will calibrate phenomenologically for optimal retrieval. Introducing a *cut* number, $\delta \in [0, 1]$, the quantum algorithm boils down to the following protocol:

- Run a number of times the circuit drawn in Figure 3 which parametrically depends on M and $t_0 = 2\pi/C$, measuring always $\sigma_z^{(n-1)}$ on the most relevant ancillary qubit.
- If $\langle \sigma_z^{(n-1)} \rangle \geq \delta$ ($\leq -\delta$) this will signal positive semi-definiteness (negative definiteness) of M . Else, if $\langle \sigma_z^{(n-1)} \rangle \in (-\delta, +\delta)$ the matrix M is classified as indefinite

Ideally we would like to send $\delta \rightarrow 1$ but this would require in turn $n \rightarrow \infty$ of the ancillary system. The optimal value of δ will need to be fixed experimentally, and we will accomplish this task in the following section.

A final word regarding the case of Hermitian matrices whose dimension is not a power of 2, so that they cannot be represented within a qubit circuit. In this case, the input matrix can be appended with vanishing lines and rows until a dimension $N = 2^m$ is reached. The random vector $|b\rangle$ will include also additional zeros in the last elements to match the correct dimension, while having vanishing projection on the appended null eigenspace.

5 Results

To check the algorithm, a sample of 1800 4x4 Hermitian matrices M has been generated. They were distributed equally over the three classes, with their eigenvalues chosen randomly and uniformly in the interval $[-1, 1)$. In the positive semi-definite class a 5% of the matrices class were forced to have one eigenvalue equal to 0.

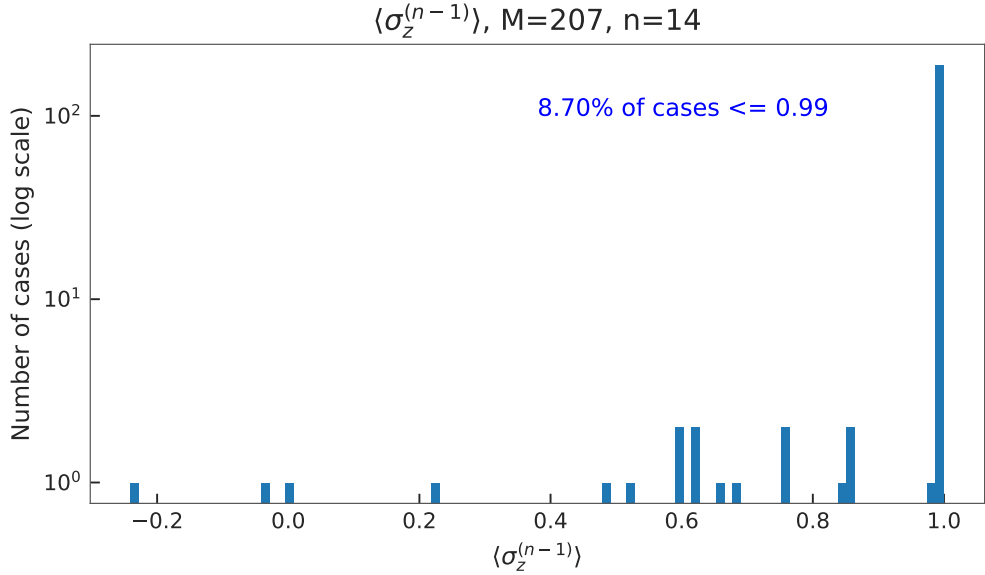


Figure 5: Results of 100 measurements for positive definite matrices

For each matrix, the full hybrid algorithm was executed taking 100 as the number of shots to compute the average value of $\langle \sigma_z^{(n-1)} \rangle$, and 5 trials for $|b\rangle$, saving the results of the trials for post-execution analysis. The algorithm was executed with $n = 4$,

Algorithm 2: Quantum classification of the definiteness of an Hermitian matrix

Input: $M \in \mathbf{C}^{N \times N}$ Hermitian Matrix
 $limitLowMin$, the lower limit for the eigenvalues
 $limitHighMax$, the higher limit for the Eigenvalues
 $Boundary$, the boundary for the classification (δ)
 $Trials$, number of trials
 n , number of qubits for the ancilla register in the QPE algorithm
 $atol$, tolerance to distinguish one number from 0
 $Shots$, number of shots for each trial

Output: Flag with class of M or Error

```

if  $M \neq M^\dagger$  then
    return Error
if ( $limitLowMin = None$ ) or ( $limitHighMax = None$ ) then
     $limitLowMin, limitHighMax \leftarrow$  using (9) and (14)
if  $dimension(M) \bmod 2 \neq 0$  then
     $d \leftarrow dimension(M)$ 
    expand M with zeros so  $dimension(M) \bmod 2 = 0$ 
 $N \leftarrow dimension(M)$ 
 $C \leftarrow 2 \max(|limitHighMax|, |limitLowMin|)$ 
 $time \leftarrow \frac{2\pi}{C}$ 
 $sigma \leftarrow 0$ 
for  $i \leftarrow 1$  to  $Trials$  do
     $\vec{b} \leftarrow$  normalized random vector  $\in C^N$  with  $N-d$  zeros at end
    Allocate ancilla register with  $n$  qubits
    Allocate  $|b\rangle$  register with  $\log(N)$  qubits
    Initialize  $|b\rangle$  to  $\vec{b}$ 
    QPE on  $M$  for  $-time$  using time evolution. (Figure 3)
     $sigma \leftarrow sigma + \langle \sigma_z^{(n-1)} \rangle$  for Shots
    classM  $\leftarrow$  Flag Indefinite
    if ( $sigma/Trials$ )  $\geq Boundary$  then
        classM  $\leftarrow$  Flag Positive Semi-Definite
    if ( $sigma/Trials$ )  $\leq -Boundary$  then
        classM  $\leftarrow$  Flag Negative Definite
    return classM

```

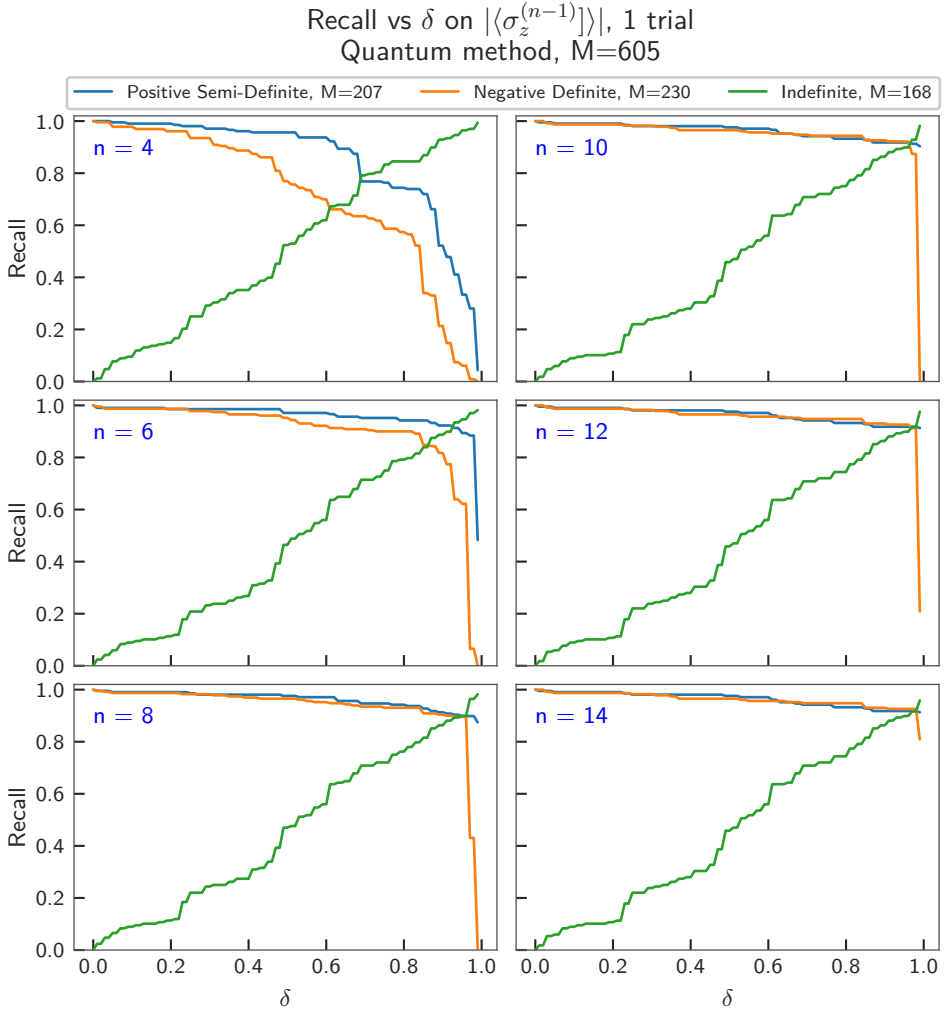


Figure 6: Recall of classification for each class for one trial.

6, 8, 10, 12 and 14 qubits on the ancilla register. It was simulated without noise using Qiskit version 0.16.1 [7], Quiskit-terra 0.12, Qiskit-aqua 0.6.4 and Qiskit-aer 0.4.1 using BasicAer *qasm_simulator* as provider. To simulate the time evolution of the Quantum Phase Estimation algorithm, the function *evolution_instruction* that implements $U(t_0)^{2^k} = (e^{-it_0 M})^{2^k}$ was used with one time slice on the Trotter-Suzuki decomposition per $U(t_0)$. This is equivalent to simulating the time evolution of the operator $U(t_0 2^k) = e^{-it_0 M 2^k}$ with 2^k time slices on the Trotter-Suzuki decomposition. A small version of the final circuit after transpilation for a 2 qubit Hermitian matrix and 2 qubit ancilla is shown in Figure 4, using barriers to show the different parts of the algorithm. The simulations were executed on CESGA FinisTerrae supercomputer between February and August of 2020, using Python 3.8.1 and Numpy 1.18.1.

Since the eigenvalues are known beforehand, we may compare the results of the classification with the actual definiteness. In Figure 5, the results for a single initialization of $|b\rangle$ are shown in the case where M is in the subset of positive definite matrices. In a 91.3% of the cases, the value of $\langle \sigma_z^{(n-1)} \rangle$ was found to be equal 1. This corresponds to having state $|0\rangle_{n-1}$ for the most relevant ancillary qubit in all of the cases, as expected for this sign-subinterval. But there is still an 8.7% of cases with values of this expectation

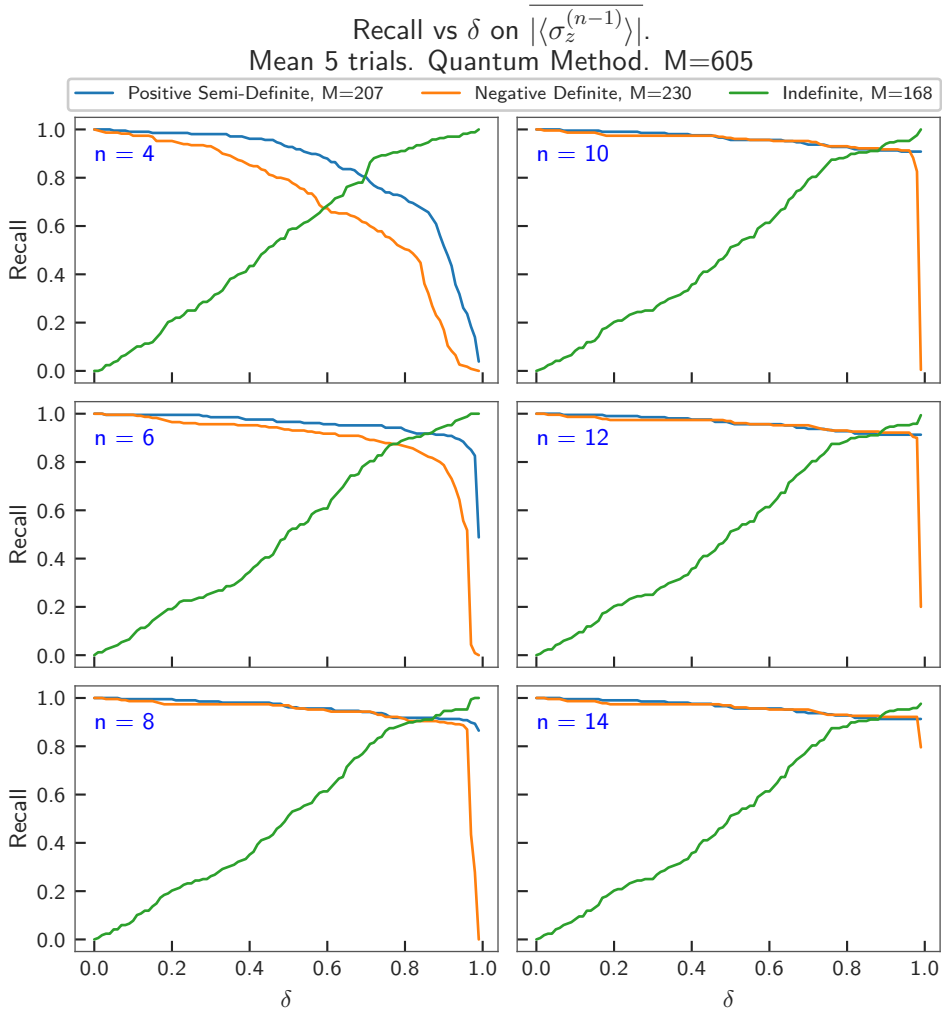


Figure 7: Recall of classification for each class for five trials.

value smaller than the maximum, meaning that some $|1\rangle_{n-1}$ states have been measured, yielding an erroneous classification. Lowering the cut, $\delta < 1$, would increase the number of correctly classified matrices.

Our task is to adjust δ so as to maximize the classification capability over all the classes. For generic M of a defined class, we will measure the ability of the algorithm to correctly classify its definiteness by using the metric $recall = \text{true positives}/(\text{true positives} + \text{false negatives})$. In Figure 6 we have plotted the behaviour of recall for the three classes as a function of the cut δ for the case of a single initialization $|b\rangle$. We notice that, as δ is lowered from its maximum value, the value of recall increases as expected for the positive semi-definite and negative definite classes. However it decreases for the class of indefinite matrices, hence a compromise value has to be searched for. The situation improves after rising the number of trials, $|b\rangle$, as shown in Figure 7. For $n \geq 12$ and 5 trials, the recall on all the classes comes very close to the maximum value in a region for $\delta \in [0, 95, 0.98]$. Our choice for $\delta = 0.98$ maximizes the *accuracy* defined as number of properly classified matrices divided by total number of matrices in the sample, reaching 92.89%. This number is roughly the average value of recall on the three classes, whose values can be seen in Table 1.

Qubits ancilla	Recall		Recall Indefinite	Accuracy(%)
	Positive	Semi-definite		
4	0.14	0.00	0.99	32.40
6	0.83	0.01	1.00	56.36
8	0.89	0.28	1.00	68.93
10	0.91	0.83	0.98	89.59
12	0.91	0.90	0.96	92.07
14	0.91	0.92	0.96	92.89

Table 1: Quantum algorithm: Recall for each class and accuracy (%) of the quantum classification versus the number of qubits on ancilla register for 5 trials and optimized cut $\delta = 0.98$.

Qubits ancilla	Recall		Recall Indefinite	Accuracy(%)
	Positive	Semi-definite		
4	0.70	0.62	1.00	77.28
6	0.94	0.62	1.00	85.33
8	0.96	0.72	1.00	89.56
10	0.97	0.93	0.99	96.50
12	0.97	0.96	0.99	97.33
14	0.97	0.97	0.99	97.61

Table 2: Hybrid algorithm: Recall for each class and accuracy (%) of the classification versus the number of qubits on ancilla register for 5 trials and optimized value of to $\delta = 0.98$.

Now we can compose the two pieces to build up the full hybrid algorithm. Running the hybrid algorithm on the sample of 1800 4x4 matrices, the classical part could correctly account for 64.67% of the positive semi-definite matrices, 64.50% of the negative cases and 71.16% of the indefinite ones. The modified curves for recall as a function of δ on the three classes for the combined hybrid algorithm can be observed in the Figure 8 for the particular case of $n = 14$ ancillary qubits. To appreciate the improvement we have added the only-quantum algorithm below. Table 2 summarizes the new values of the recalls and global accuracy for the selected value $\delta = 0.98$ again for $n = 14$ for comparison with Table 1. The global accuracy increases up to 97.61% with the hybrid algorithm. These numbers illustrates the advantage of combining both procedures into a more powerful hybrid algorithm.

Finally the importance of initializing with more than one vector $|b\rangle$ is shown in Figure 10. As a matter of fact this plot reveals g beyond 3 independent vectors no significant improvement is obtained. We then checked that initializing with the three independent vectors $|0\rangle^n, |1\rangle^n$ and $H^n |0\rangle^n$ performs as good as with random vectors and is much faster to implement.

6 Discussion and further work

We have described a hybrid algorithm to classify Hermitian matrices according to its definiteness. We believe it brings in a quantum advantage over its classical counterparts. It is also fair to recognize the shortcomings of the algorithm. It is probabilistic, although the achieved accuracy values easily reaches 97%. Another criticism may say that initially the Quantum part cannot distinguish between positive and positive semi-definite cases. This limitation can be easily overcome by running the algorithm a second time, now for the negative matrix $M' = -M$. If the M' is classified as negative definite (indefinite), the

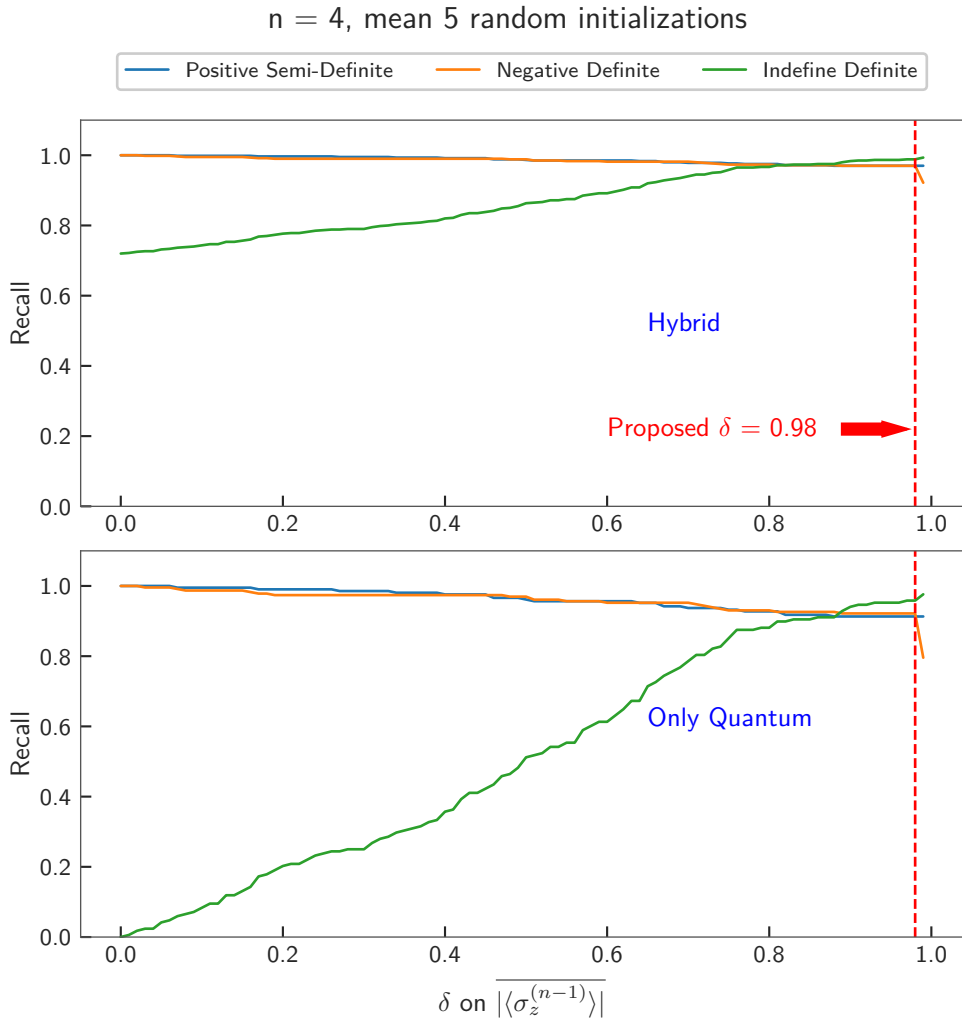


Figure 8: Classification boundary for 5 trials. Top, recall of hybrid algorithm. Bottom, recall of only quantum version.

original matrix M is positive definite (positive semi-definite). For the Quantum Algorithm just a time sign change $t = -2\pi/C \rightarrow 2\pi/C$ is needed, and even it can be made in parallel. In future work, this improvement will be explored and evaluated.

An analysis of the computational cost of the algorithm is important in order to evaluate the possible quantum advantage. Classical methods in the literature have a computational cost, as said before, of $O(N^{w+1})$ for generic matrices, being N the dimension of the Hermitian matrix, when all the eigenvalues need to be calculated, and in specific cases, $O(N^3)$.

In our case, in the $\sim 65\%$ of cases where the classical stage correctly classifies M , this brings in a substantial improvement in the performance, because only $O(N^2)$ operations are needed. The price of course is the low overall accuracy and this is where the quantum addendum plays a role.

The quantum part of the algorithm consists of three main parts: the initialisation of the state $|b\rangle$, the unitary time evolutions, and the QFT, both implicit in the QPE protocol.

The initialisation of the state $|b\rangle$ in the case of matrices with dimensions $N = 2^m$ can be done using $m = O(\log(N))$ operations and similar order when the dimension of the

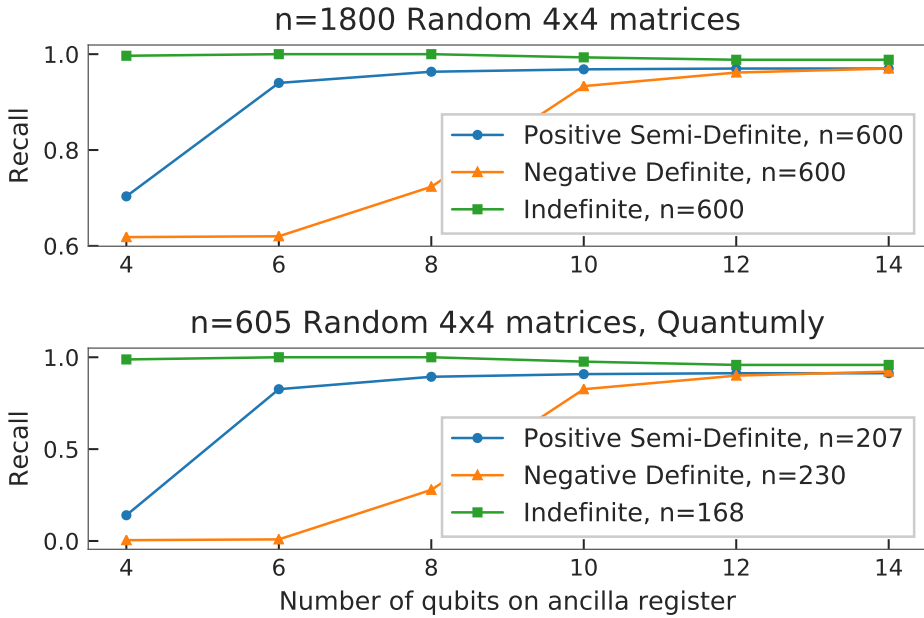


Figure 9: Recall of the classification for each class versus the number of ancillary qubits for random Hermitian matrices $\in C^{4 \times 4}$. Top, the results of the hybrid algorithm, including classical and quantum part. Bottom, the results of the fraction of the matrices which were classified using the quantum algorithm.

matrix is not a power of two. The computational cost of the inverse of the QFT depends on the implementation, but in some cases can be done in $O(n \log(n))$, being n the number of qubits of the ancilla register, and is independent of the dimension of the matrix.

As said, we will need to implement n unitary evolutions $U(t_0 2^k) = e^{-it_0 M 2^k}$, $k = 0, \dots, n-1$. For each one of them, the Trotter-Suzuki decomposition has been chosen to be in 2^k uniform time slices. The possible effect of refining this slicing must be studied with care because the eventual improvement in performance comes at the cost of a significant increase in execution time. The main contribution to the scaling of the computational complexity comes from implementing the time evolution. Nowadays, algorithms to compute it for an Hermitian matrix start by decomposing it into combinations of tensor products of Pauli matrices. For a matrix of dimension N , there are $4^{\log_2(N)} = N^2$ possible terms in this decomposition, and obtained by calculating the trace of the product of each Pauli combination with the matrix. Because any possible tensor product of Pauli's operators has N non-zero elements, the number of operations to prepare the matrix is $O(N 4^{\log_2(N)}) = O(N^3)$. To implement this decomposition on a computable circuit, a maximum of $2(\log_2(N) - 2)$ CNOT gates and another $(2\log_2(N) - 1)$ rotations are needed [8]. This circuit must be executed $O(2^n)$ times. Putting all together, the computational complexity is $O(N 4^{\log_2(N)} + 2^{n+2} \log_2(N) 4^{\log_2(N)})$, that it is dominated by the first term, i.e., the computational complexity on the current situation of the technology grows as $O(N^3)$ for fixed ancillary system.

As consequence, the actual quantum algorithm has a computational complexity that improves the actual classical algorithms, but is worse than the classical theoretical limit. Let us digress now and speculate about the theoretical limit on the complexity of the quantum algorithm. Certainly the bulk of the complexity stems from the computational cost of the quantum implementation of an arbitrary rank N unitary operator. We mention

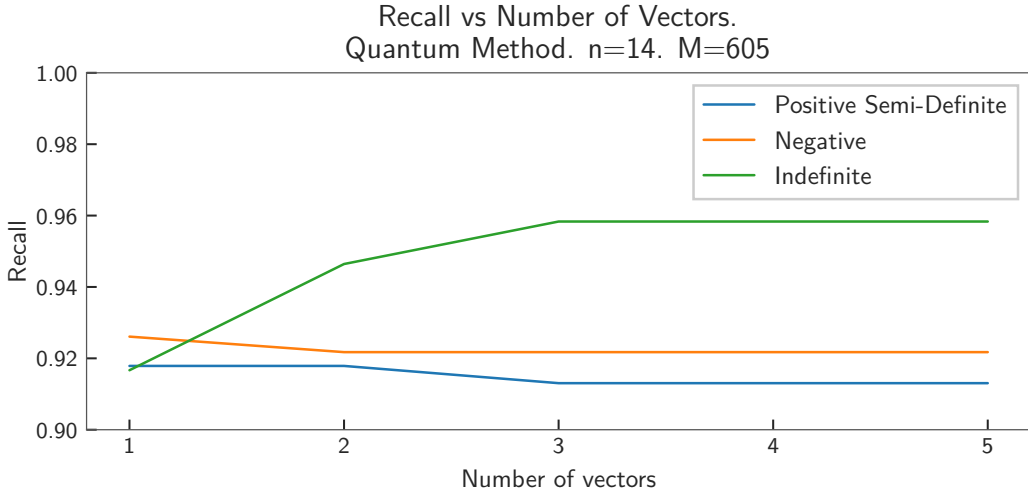


Figure 10: Behavior of Recall vs. the number of initialization trials $|b\rangle$. We observe that 3 seems to be the optimal value and going beyond does not bring in any improvement.

some results in the literature that hint towards the possibility of improving over the ones expressed above. For the case of a Universal Quantum Computer, Shende et al. [9] demonstrated that any unitary operator can be implemented on a quantum circuit containing no more than $O(N^2)$ CNOT gates. More specifically, referring to the case of a Trapped Ion Computer, Goubault De Brugi  re et al. [10] have shown that almost any unitary operation requires a number of gates ² that is bounded by

$$\#Gates \geq (4m + 1) \left\lceil \frac{4^m - 3m - 1}{2m + 1} \right\rceil + 5m \approx O(N^2). \quad (18)$$

These results point out towards the possibility of finding a bound for the computational cost of the quantum part of our algorithm below the naive counting $\mathcal{O}(N^3)$.

In summary, the algorithm is composed of a classical part with lower computational complexity than the known classical algorithms which can solve around 65% of the cases, and a quantum part that, in the current state of the technology, is not worse than the classical one, but has still room for improvement. The quantum algorithm uses efficiently the quantum parallelism and state measurement. Its gain in performance severely depends on the possibility of reducing the number of gates needed to implement the time evolution operator of a generic Hermitian matrix.

7 Acknowledgements

Authors want to thank CESGA for the provision of the computing resources, specially for the computing time on FinisTerrae II. Also, authors have used extensively the computing resources integrated in this supercomputer from Instituto Gallego de F  sica de Altas Energ  as (IGFAE). Those resources have been funded by Axencia Galega de Innovaci  n (GAIN). Without them, this work would not have been possible. We also appreciate the

²In Trapped Ion Computers the universal set of gates is composed of local $R_z(\varphi)$ and $R_x(\theta)$ gates, and the entangling M  lmer-S  rensen gate defined by $MS(\theta) = e^{-i\theta(\sum_{i=0}^m \sigma_x^i)^2/4}$.

comments from Cyril Allouche and Timothee Goubault de Brugiere from ATOS, which help to improve the content significantly, and from Juan José Nieto Roig from University of Santiago de Compostela. The work of JM was supported by grants FPA2014-52218-P and FPA2017-84436-P from Ministerio de Economía y Competitividad, by Xunta de Galicia ED431C 2017/07, by FEDER and by Grant María de Maeztu Unit of Excellence MDM-2016-0692.

References

- [1] Jorge Nocedal and Stephen J Wright. *Numerical Optimization*. Springer-Verlag, New York, 1999.
- [2] Carl D. Meyer. *Numerical Optimization*. SIAM-Philadelphia, New York, 2000, Section 7.6.
- [3] John E. Prussing. The principal minor test for semidefinite matrices. *Journal of Guidance, Control, and Dynamics*, 9(1):121–122, jan 1986.
- [4] Victor Y. Pan and Zhao Q. Chen. The complexity of the matrix eigenproblem. In *Proceedings of the thirty-first annual ACM symposium on Theory of computing - STOC '99*, pages 507–516, New York, New York, USA, 1999. ACM Press.
- [5] Michael A Nielsen and Isaac Chuang. Quantum computation and quantum information, 2002.
- [6] Henry Wolkowicz and George P.H. Styan. Bounds for eigenvalues using traces. *Linear Algebra and its Applications*, 29:471–506, feb 1980.
- [7] Héctor Abraham, AduOffei, Ismail Yunus Akhalwaya, Gadi Aleksandrowicz, Thomas Alexander, Gadi Alexandrowics, Eli Arbel, Abraham Asfaw, Carlos Azaustre, AzizNgoueya, Panagiotis Barkoutsos, George Barron, Luciano Bello, Yael Ben-Haim, Daniel Bevenius, Lev S. Bishop, Sorin Bolos, Samuel Bosch, Sergey Bravyi, David Bucher, Fran Cabrera, Padraig Calpin, Lauren Capelluto, Jorge Carballo, Ginés Carrascal, Adrian Chen, Chun-Fu Chen, Richard Chen, Jerry M. Chow, Christian Claus, Christian Clauss, Abigail J. Cross, Andrew W. Cross, Simon Cross, Juan Cruz-Benito, Chris Culver, Antonio D. Córcoles-Gonzales, Sean Dague, Tareq El Dandachi, Matthieu Dartailh, DavideFrr, Abdón Rodríguez Davila, Delton Ding, Jun Doi, Eric Drechsler, Drew, Eugene Dumitrescu, Karel Dumon, Ivan Duran, Kareem EL-Safty, Eric Eastman, Pieter Eendebak, Daniel Egger, Mark Everitt, Paco Martín Fernández, Axel Hernández Ferrera, Albert Frisch, Andreas Fuhrer, MELVIN GEORGE, Julien Gacon, Gadi, Borja Godoy Gago, Jay M. Gambetta, Adhisha Gammanpila, Luis García, Shelly Garion, Juan Gomez-Mosquera, Salvador de la Puente González, Jesse Gorzinski, Ian Gould, Donny Greenberg, Dmitry Grinko, Wen Guan, John A. Gunnels, Mikael Haglund, Isabel Haide, Ikko Hamamura, Vojtech Havlicek, Joe Hellmers, Łukasz Herok, Stefan Hillmich, Hiroshi Horii, Connor Howington, Shaohan Hu, Wei Hu, Haruki Imai, Takashi Imamichi, Kazuaki Ishizaki, Raban Iten, Toshinari Itoko, JamesSeaward, Ali Javadi, Ali Javadi-Abhari, Jessica, Kiran Johns, Tal Kachmann, Naoki Kanazawa, Kang-Bae, Anton Karazeev, Paul Kassebaum, Spencer King, Knabberjoe, Arseny Kovyrshin, Rajiv Krishnakumar, Vivek Krishnan, Kevin Krsulich, Gawel Kus, Ryan LaRose, Raphaël Lambert, Joe Latone, Scott Lawrence, Dennis Liu, Peng Liu, Yunho Maeng, Aleksei Malyshev, Jakub Marecek, Manoel Marques, Dolph Mathews, Atsushi Matsuo, Douglas T. McClure, Cameron McGarry, David McKay, Dan McPherson, Srujan Meesala, Martin Mevissen, Antonio Mezzacapo, Rohit Midha, Zlatko Minev, Abby Mitchell, Nikolaj Moll, Michael Duane Mooring, Renier Morales, Niall Moran, MrF, Prakash Murali, Jan Müggenburg, David Nadlinger,

Ken Nakanishi, Giacomo Nannicini, Paul Nation, Edwin Navarro, Yehuda Naveh, Scott Wyman Neagle, Patrick Neuweiler, Pradeep Niroula, Hassi Norlen, Lee James O’Riordan, Oluwatobi Ogunbayo, Pauline Ollitrault, Steven Oud, Dan Padilha, Hanhee Paik, Simone Perriello, Anna Phan, Francesco Piro, Marco Pistoia, Alejandro Pozas-iKerstjens, Viktor Prutyanov, Daniel Puzzuoli, Jesús Pérez, Quintiii, Rudy Raymond, Rafael Martín-Cuevas Redondo, Max Reuter, Julia Rice, Diego M. Rodríguez, RohithKarur, Max Rossmannek, Mingi Ryu, Tharrmashastha SAPV, Sam-Ferracin, Martin Sandberg, Hayk Sargsyan, Ninad Sathaye, Bruno Schmitt, Chris Schnabel, Zachary Schoenfeld, Travis L. Scholten, Eddie Schoute, Joachim Schwarm, Ismael Faro Sertage, Kanav Setia, Nathan Shammah, Yunong Shi, Adenilton Silva, Andrea Simonetto, Nick Singstock, Yukio Siraichi, Iskandar Sittikov, Seyon Sivaramah, Magnus Berg Sletfjerdning, John A. Smolin, Mathias Soeken, Igor Olegovich Sokolov, SooluThomas, Dominik Steenken, Matt Stypulkoski, Jack Suen, Shaojun Sun, Kevin J. Sung, Hitomi Takahashi, Ivano Tavernelli, Charles Taylor, Pete Taylour, Soolu Thomas, Mathieu Tillet, Maddy Tod, Enrique de la Torre, Kenso Trabing, Matthew Treinish, TrishaPe, Wes Turner, Yotam Vaknin, Carmen Recio Valcarce, Francois Varchon, Almudena Carrera Vazquez, Desiree Vogt-Lee, Christophe Vuillot, James Weaver, Rafal Wieczorek, Jonathan A. Wildstrom, Robert Wille, Erick Winston, Jack J. Woehr, Stefan Woerner, Ryan Woo, Christopher J. Wood, Ryan Wood, Steve Wood, James Wootton, Daniyar Yeralin, Richard Young, Jessie Yu, Christopher Zachow, Laura Zdanski, Christa Zoufal, Zoufalc, a matsuo, azulehner, bcamorrison, brandhsn, chlorophyll zz, dan1pal, dime10, drholmie, elfrocampedor, faisaldebouni, fanizzamarco, gadial, gruu, kanejess, klinvill, kurarrr, lerongil, ma5x, merav aharoni, michelle4654, ordmoj, sethmerkel, strickroman, sumitpuri, tigerjack, toural, vvilpas, welien, willhbang, yang.luh, yelojakit, and yotamvakninibm. Qiskit: An open-source framework for quantum computing, 2019.

- [8] Kaiwen Gui, Teague Tomesh, Pranav Gokhale, Yunong Shi, Frederic T Chong, Margaret Martonosi, and Martin Suchara. Term Grouping and Travelling Salesperson for Digital Quantum Simulation. *Arxiv:2001.05983*, jan 2020.
- [9] Vivek V Shende, Stephen S Bullock, and Igor L Markov. Synthesis of Quantum Logic Circuits. *arXiv:quant-ph/0406176v5*, 2006.
- [10] Timothée Goubault De Brugièr, Marc Baboulin, Benoît Valiron, and Cyril Allouche. Synthesizing quantum circuits via numerical optimization. *Arxiv:2004.07714v1*, 2020.